Nuclear Engineering and Technology 52 (2020) 2847–2851

Contents lists available at ScienceDirect

Nuclear Engineering and Technology

journal homepage: www.elsevier.com/locate/net

Original Article

On-site water level measurement method based on wavelength division multiplexing for harsh environments in nuclear power plants

Hoon-Keun Lee [a], Jaeyul Choo [b], Gangsig Shin [a], Sung-Man Kim [c,*]

[a] Department of Safety Research, Korea Institute of Nuclear Safety, 62 Gwahak-ro, Yuseong-gu, Daejeon, 34142, South Korea
[b] Department of Instrumentation, Control and Electrical System, Korea Institute of Nuclear Safety, 62 Gwahak-ro, Yuseong-gu, Daejeon, 34142, South Korea
[c] Department of Electronic Engineering, Kyungsung University, Nam-Gu, Busan, 48434, South Korea

ARTICLE INFO

Article history:
Received 28 January 2020
Received in revised form
29 April 2020
Accepted 6 May 2020
Available online 15 June 2020

Keywords:
Spent fuel pool
Water level measurement
Optical fiber sensor
Wavelength division multiplexing

ABSTRACT

A simple water level measurement method based on wavelength division multiplexing (WDM) is proposed and demonstrated. The measurement principle is based on the change of Fresnel reflection occurring at the end facet of the optical fiber tip (OFT). To increase the spatial resolution of water level sensing, a broadband light source (BLS) and an arrayed waveguide grating (AWG) are employed. The OFTs are multiplexed with the dedicated wavelength channels of AWG. By measuring all of the reflection powers reflected at the OFTs with a proposed on-site reflectometer, the water level can be monitored continuously for a fast emergency response. Moreover, it can be implemented easily with the commercially available optical components and devices with the simple configuration.

Water level is one of the essential parameters for many industrial areas related to the environmental safety. Especially, in spent fuel pools (SFPs) of nuclear power plants, water plays an important role in cooling down of decay heat and shielding of the radiation fields [1]. Until now, various water level sensing techniques have been proposed based on optical fiber sensors (OFSs) for the harsh environment such as high temperature, gamma radiation and so on [2,3]. The OFS provides many advantages such as passive sensing capability, remote sensing, resistance to electro-magnetic interference and radiation [4]. For the water level measurement, it is generally divided into two types: continuous level sensors and discrete (or quasi-distributed) level sensors. The continuous level sensors provide quantitative information of the water level in a range of specific area with a high spatial resolution continuously. It can be implemented based on the long-period fiber grating [5], etched D-shape optical fiber [6], no core fiber [7], heated fiber with an insulated heat wire [8], and so on. However, these methods require the use of a special fiber structure, an additional heating device, or complex signal processing techniques based on optical frequency domain reflectometry. On the other hands, the discrete level sensors simply detect the presence of the water according to the previously designed installation position with an optical coupler [1,9,10]. The multiple discrete sensors can be multiplexed on a single fiber to provide quasi-distributed sensing performance [11–13]. However, the multi-channel sensing capability is limited fundamentally due to its insertion loss of the optical coupler or the complex fabrication process for multiplexing the multiple discrete sensors.

Recently, we proposed a simple all-optical water level monitoring system based on the wavelength division multiplexing (WDM) technique for SFPs in nuclear power plants [14]. This system provides the simplest way for multi-channel sensing, a high spatial resolution, and robustness to external temperature changes at a remote location with a remote reflectometer. However, the single mode fiber can be possibly damaged due to the external event such as the Fukushima-Daiichi accident, and it can result in the loss of the reflected signal which containing the information of water level. To handle this problem, one of the simplest approaches is for operators to access an equipment room where the AWG is installed and measure the reflected optical power with a hand-held type on-site reflectometer. Since, the previously proposed remote reflectometer is employing a commercial optical spectrum analyzer (OSA) for water level measurement, it is difficult for operators to carry it from the main control room in an emergency situation for a nuclear power plant.

* Corresponding author.
E-mail address: sungman@ks.ac.kr (S.-M. Kim).

https://doi.org/10.1016/j.net.2020.05.005

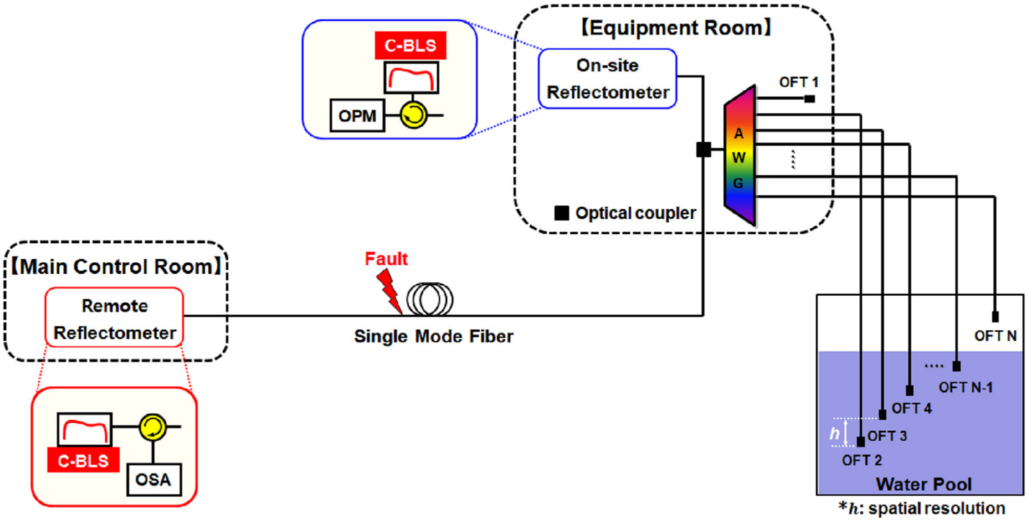

Fig. 1. Configuration of the proposed water level monitoring system based on wavelength division multiplexing.

In this letter, we propose a very simple water level measurement method based on the WDM technique with an on-site reflectometer for a fast emergency response. For the purpose of multiplexing, it utilizes a broadband light source (BLS) and an arrayed waveguide grating (AWG). By measuring the total reflection power resulting from the optical fiber tips (OFTs) depending on the presence of the water, the water level can be detected easily with an optical power meter (OPM). Above all, the proposed scheme can be implemented easily with the commercially available optical components and devices.

Fig. 1 shows the architecture of the proposed on-site water level monitoring system. It consists of an on-site reflectometer for power measurement of the reflected optical signal, a 1 × N AWG for channel multiplexing/de-multiplexing, and OFTs for sensing the water presence. As shown in the inset of Fig. 1, the on-site reflectometer consists of a C-BLS based on ASE (amplified spontaneous emission), an optical circulator and an OPM. The ASE light for BLS is generated by a pumped erbium-doped fiber. It can provide a large bandwidth (more than 30 nm) with the gain-flattened output spectrum (2.5-dB power deviation at maximum) [14]. For the measurement of total reflected optical power at the on-site location, the proposed reflectometer is designed for portable use. By accessing the equipment room, the reflectometer is connected to one of the optical coupler ports.

The basic principle of water level sensing is based on the Fresnel reflection occurring at the OFTs due to the change of refractive index [14]. The OFT is based on a single mode fiber including the standard SC/PC type connectors with a ceramic ferrule diameter of 2.5 mm at the ends of the fiber. Fig. 2(a) and (b) show the schematic diagrams of the OFTs and measured optical spectra at 1550 nm according to the Fresnel reflection in the air and water, respectively. The Fresnel reflection power coefficient (R_m) at the OFT is given by

$$R_m = \left(\frac{n_f - n_m}{n_f + n_m}\right)^2 \tag{1}$$

where n_f and n_m correspond respectively to the refractive index of the fiber and surrounding materials (n_a for air, n_w for water) at the end facet of the fiber tip. For the calculation of R_m, we assumed the refractive index of the fiber is 1.4492, air is 1.0002739, and water is 1.3152 at 10 °C [15–17]. Moreover, these values can be approximated by constants within C-band regardless of wavelength and temperature dependence [14]. The theoretical values of the Fresnel reflection power coefficient are about −26.3 dB (0.23%) in the water (R_{water}) and −14.7 dB (3.36%) in the air (R_{air}), respectively. The reflected power difference (ΔP) between R_{air} and R_{water} is 11.6 dB as shown in Fig. 2(b).

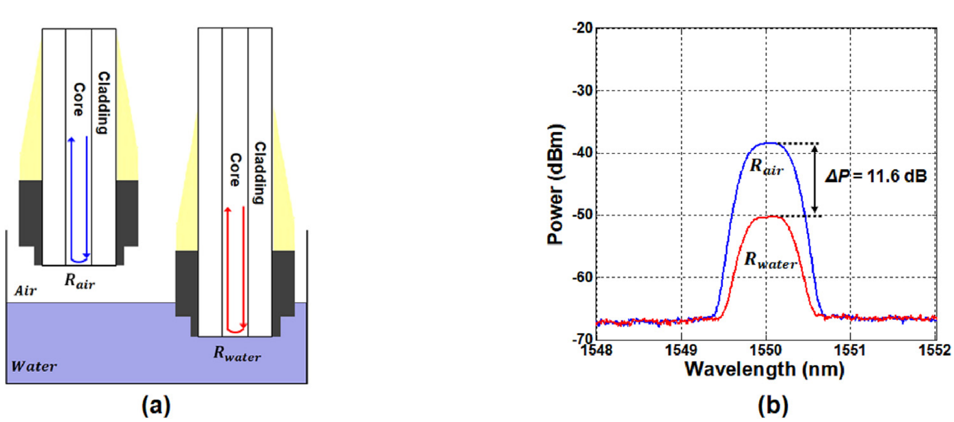

Fig. 2. (a) Schematic diagrams of the OFT and (b) measured spectra according to the refractive indices of materials (R_{air} : reflection in the air, and R_{water}: reflection in the water).

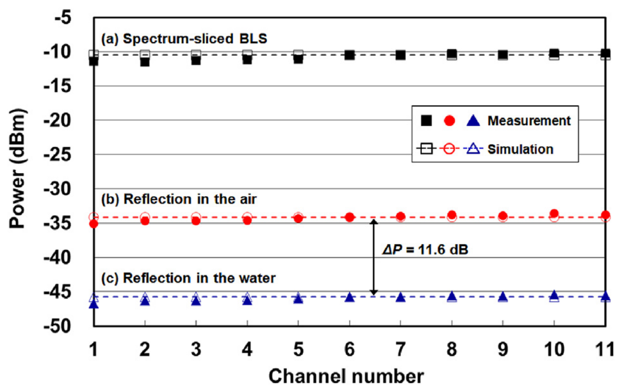

Fig. 3. Measurement and simulation values of the received optical power at each of the 11 AWG channels (a) spectrum-sliced BLS (b) reflection in the air (c) reflection in the water.

To check a multi-channel sensing capability, we also measured the reflected power difference between two materials for the 11 channels of AWG. Fig. 3(a) shows the received optical power of the BLS which is spectrally sliced by the AWG, and Fig. 3(b), (c) show the received optical powers reflected from the air and water according to the channels, respectively. The measurement results presented similar reflection characteristics in each channel, and these results (solid marks) were well matched with the simulation results (hollow marks). Thus, by measuring the total optical powers reflected from the OFTs installed in a water pool, the current status of the water level can be easily monitored in a real-time for a rapid emergency response.

Next, it is important to compare the optical received powers to the optical spectra depending on the water levels to verify the feasibility of the proposed method. The intensity of the received optical spectrum in front of the on-site reflectometer can be expressed as Eq. (2) [14].

$$I_{output}(\lambda)\ [W] = 10^{\left(-\frac{L_{IL}}{10}\right)} \cdot R_m \cdot |E_{ASE}(\lambda)|^2 \cdot \left|\sqrt{T_{AWG}(\lambda)}\right|^4 \tag{2}$$

Here, $E_{ASE}(\lambda)$ and $T_{AWG}(\lambda)$ correspond to the electrical field of BLS based on ASE light and the AWG transfer function, respectively. The AWG can be modeled as a series of band-pass filters with a Gaussian passband:

$$T_{AWG}(\lambda) = \sum_{i=1}^{N} exp\left[-ln2\left(\frac{|\lambda-\lambda_i|}{\Delta\lambda_{BW}}\right)^{2m}\right] \tag{3}$$

where i is the channel number, N is total number of channels, and λ_i is the center wavelength of each AWG channel which has a channel spacing between the adjacent channels. $\Delta\lambda_{BW}$ is the 3 dB bandwidth of each channels, and m represent the filter order for super-Gaussian shape at each channels, respectively. The parameter values for AWG are m of 1.415, $\Delta\lambda_{BW}$ of 0.64 nm, and the channel spacing of 0.8 nm. Next, the parameter of L_{IL} in Eq. (2) represents the total insertion loss of the signal reflection path in dB scale, and it can be expressed with below Eq. (4) for the proposed scheme based on the on-site reflectometer.

$$L_{IL}[dB] = 2\left(L_{OC} + L_{AWG} + L_{OFT} + L_{Coupler}\right) \tag{4}$$

where L_{OC}, L_{AWG}, L_{OFT}, and $L_{Coupler}$ represent the insertion losses of the optical circulator, AWG, OFT, and optical coupler, respectively. For the simulation, we estimated L_{OC} of 1.5 dB, L_{AWG} of 4.5 dB, and L_{OFT} of 1 dB. These insertion losses are based on the measurement results. Here, the optical coupler is not included in the experiment setup for demonstration. Based on the above equations, the total reflected optical power can be calculated by integrating the received optical intensity within the interested wavelength band. It should be noted that the fiber length between the equipment room and the spent fuel pool is considered to be within a few tens of meter maximally, so that the Rayleigh backscattering effect resulting from the transmitted BLS can be negligible [18].

In this experiment, we demonstrated the proposed scheme for 11 channels of AWG with the C-band due to the limitation of the experimental equipment. We utilized 10 nm wavelength band (1545–1555 nm) of the BLS with the help of the optical band-pass filter. The measured total BLS power was about +6 dBm (OSA: −11.2 dBm/0.2 nm) after passing the optical circulator. The BLS output was spectrum-sliced by the flat-top passband AWG. The channel spacing and 3 dB bandwidth of the AWG were about 0.8 nm (100 GHz) and 0.64 nm (80 GHz), respectively. For the channel 6 of the AWG (center wavelength: 1550 nm), the measured spectrum-sliced BLS power was about −10.5 dBm (OSA: −15.7 dBm/0.2 nm). The OFTs were connected with the 11 channels of the AWG, and their lengths and losses of the OFTs were about 2 m and within 1 dB, respectively. The tips were immersed in a tank filled with the water of about 10 °C and the height of the water tank was about 30 cm. It should be noted that the proposed method is utilizing the existing passive equipment (such as the AWG and OFTs) that are already installed for remote sensing with the remote reflectometer. Thus, in this configuration, the two channels of the AWG (channel 1 for primary and 11 for back-up) still function as the reference channels which measure only the optical powers reflected from the air.

Fig. 4 shows the measured and simulated optical spectra of 11 WDM channels in front of the on-site reflectometer at the full water level (a), the medium level (b), and the lowest water level (c), respectively. The experimental results show a good agreement with the simulation results. The BLS output spectrum was measured after passing through the optical circulator. As mention above, this proposed method is utilizing the legacy water level monitoring system for remote sensing, the 9 sensing channels (ch2~10) can be used to identify the presence of the water according to the specified installation positions. Thus, in this demonstration, the 10 steps of water level can be presented with the 9 sensing channels from the lowest level of 0 step (1/111 111 111/1) to the highest level of 9 step (1/000 000 000/1). Here, '0' and '1' levels indicate the presence and absence of water according to the AWG channels such as digital signal modulation, respectively. Moreover, the number of sensing channels is related with the spatial resolution of the measurement system. The spatial resolution (h) of water level can be represented with below equation,

$$h = H/(N-1) \tag{5}$$

where H is the total interesting height of the pool and N is the number of AWG channels, respectively. For example, a 32 channel AWG is selected for water level measurement with the 9 m depth of water pool, the spatial resolution becomes about 0.3 m. It may be noted that this resolution is enough to meet the minimum resolution requirement for SFP [19].

Next, we measured the reflected optical power depending on the water level with the OPM. As shown in Fig. 5, it is observed that the received optical power decreases with the increase of water level due to the increasing of the number of OFTs submerged in the water. The simulation results are also plotted to compare with the experimental results. In this figure, the maximum power difference between the experiment and the simulation (ideal case) results is

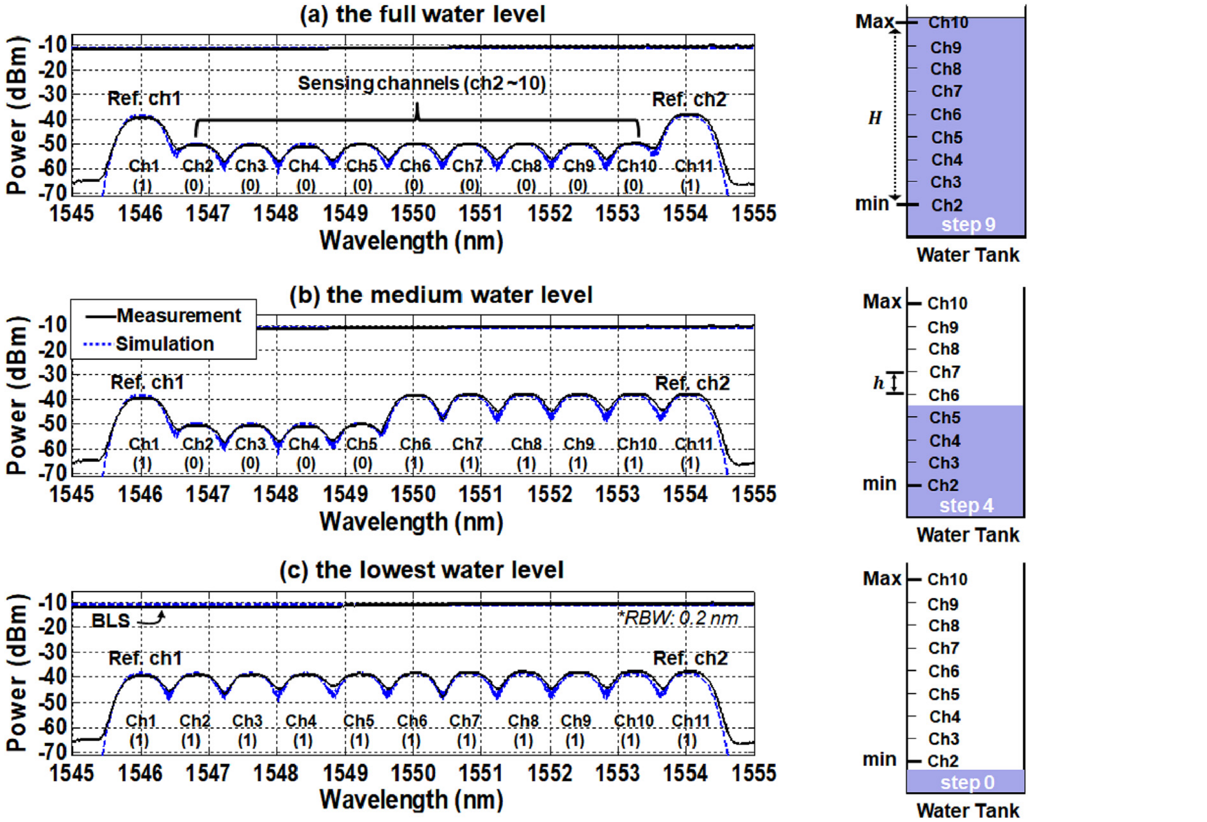

Fig. 4. Measured and simulated optical spectra of 11 WDM channels according to the water level: (a) the full water level, (b) the medium water level, and (c) the lowest water level.

less than 0.3 dB. This power difference can be attributed to a variety of factors depending on the channels, such as the different insertion losses (including the AWG, OFT) and the spectral profile of the BLS output. Moreover, these factors are also related to the linear characteristic of the sensor system. Thus, when designing the sensor system based on WDM, these components should be carefully selected to guarantee the linearity. To illustrate the sensor's linearity, the linear fitting curve ($y = b_1x + b_0$) is represented based on the experimental data. The linear fit curve has the slope (b_1) of -0.3588 and the intercept (b_0) of 4.6187, respectively. The coefficient of determination (R^2) for the linear fit is 0.998 and it shows an excellent linear response characteristic.

In addition, we investigated the effect of temperature variation in the water with simulation. This is because the water temperature in a spent fuel pool can be changed by the external environmental condition such as a trip of recirculation cooling pump [14]. For this simulation, we assumed the reflective indices of water which are 1.3118 at 40 °C, 1.3060 at 70 °C, and 1.2977 at 100 °C, respectively [17]. These simulation results are also shown in Fig. 5. The higher the water level, the greater the variation in total received power due to changes in the temperature of the water. This is because the number of the OFTs which is submerging in the water also increases. The inset of Fig. 5 represents the enlargement part of the received optical power according to temperature at the highest water level of step 9 (1/000 000 000/1), and the maximum power variation (ΔP_{temp}) is only about 0.3 dB. It should be noted that the power difference between the water level of step 8 and 9 is about 1.3 dB. Thus, it can be negligible the effect of temperature changes in the water for level measurement.

In summary, we have proposed and experimentally demonstrated a very simple water level measurement method based on WDM. The implemented WDM sensor system provides an excellent linear response with an enhanced spatial resolution, and

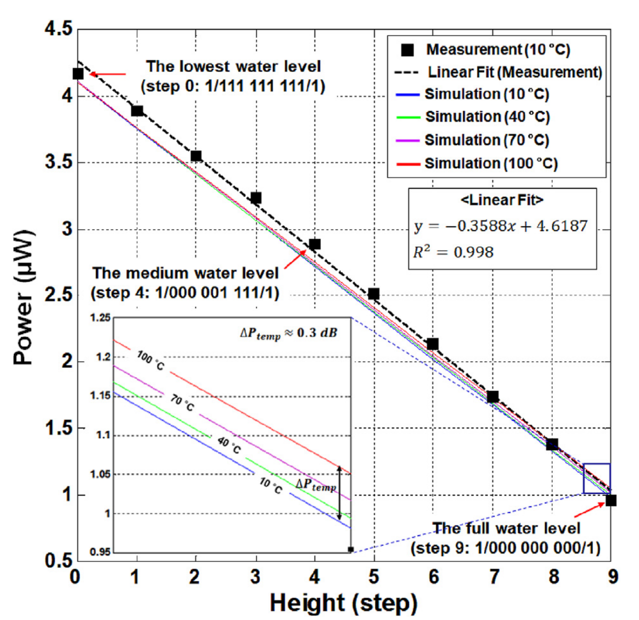

Fig. 5. Measured and simulated optical power according to the water level. The inset shows the enlargement part of the received optical power according to temperature at the highest water level (step 9).

robustness on the temperature variation of water. Moreover, it can be implemented easily with commercially available optical components and devices for the purpose of on-site measurement. It is expected that the proposed method could be applied as an auxiliary monitoring system for a spent fuel pool to response emergency situation.

Unlike the time division multiplexing (TDM) method [1], the proposed WDM technique has lots of advantages for the water level measurement. First, the WDM can increase the spatial resolution (h) for water level easily compared to the TDM, by reducing the channel bandwidth of the AWG. Because of the high insertion loss of optical coupler, there is a limitation to expand the number of channel ports in the TDM-based method. Second, it does not need any careful consideration for optical fiber length related to a delayed time of the reflected light according to the channels. As a result, it can enhance the efficiency of maintenance with the reduced cost.

In spite of these merits, the contact type of OFTs can be affected by the floating particles (such as dust) or small particles dissolved in the water. These particles can cause the performance degradation by adhering to the end facets of OFTs. However, it can be mitigated considerably by the purification system of SFP. This purification function is carried out through one or two flow paths to prevent corrosion of spent fuels and related facilities. These flow paths are consisting of floating removal filters, ion exchangers and so on. Even if the water quality is maintained through the purification system, some contamination materials can be attached on the surfaces of the OFTs over time. One of the simple solution is to replace the contaminated OFT with a new one. To facilitate this maintenance activity, each OFT needs to be divided into two sections with an optical connector. Thus, by replacing the section that the OFTs are submerged into the water for level sensing at every certain period of time, the system performance can be maintained for a long time. A periodic test with the optical spectrum analyzer will be helpful to monitor the condition of each OFT for determination of the replacement cycle.

Declaration of competing interest

The authors declare that they have no known competing financial interests or personal relationships that could have appeared to influence the work reported in this paper.

Acknowledgements

This research was partially supported by the National Research Foundation of Korea (NRF) grant funded by the Korea government (MSIT) (No. 2019R1F1A1045956).

References

[1] W.J. Yoo, H.I. Sim, S.H. Shin, K.W. Jang, S. Cho, J.H. Moon, B. Lee, A fiber-optic sensor using an aqueous solution of sodium chloride to measure temperature and water level simultaneously, Sensors 14 (2014) 18823–18836.
[2] S. Rizzolo, J. Périsse, A. Boukenter, Y. Ouerdane, E. Marin, J.-R. Macé, M. Cannas, S. Girard, Real time monitoring of water level and temperature in storage fuel pools through optical fibre sensors, Sci. Rep. 7 (2017), https://doi.org/10.1038/s41598-017-08853-7.
[3] A. Stancălie, F. Esposito, R. Ranjan, P. Bleotu, S. Campopiano, A. Iadicicco, D. Sporea, Arc-induced Long Period Gratings in standard and speciality optical fibers under mixed neutron-gamma irradiation, Sci. Rep. 7 (2017), https://doi.org/10.1038/s41598-017-16225-4.
[4] P. Ferdinand, S. Magne, G. Laffont, Optical fiber sensors to improve the safety of nuclear power plants, in: Proc. Of the Fourth Asia Pacific Optical Sensors Conference, 2013. Wuhan, China, October 15-18.
[5] S. Grice, W. Zhanga, K. Sugdena, I. Benniona, Liquid level sensor utilising a long period fiber grating, in: Proc. Of Optical Components and Materials VI, United State, San Jose, CA, 2009. February 4-6.
[6] S.M. Chandani, N.A.F. Jaeger, Optical fiber-based liquid level sensor, Opt. Eng. 46 (2007), 114401, 1–114401-7.
[7] J.E. Antonio-Lopez, J.J. Sanchez-Mondragon, P. LikamWa, D.A. May-Arrioja, Fiber-optic sensor for liquid level measurement, Opt. Lett. 36 (2011) 3425–3427.
[8] C.M. Petrie, J.L. McDuffee, Liquid level sensing for harsh environment applications using distributed fiber optic temperature measurements-heating, Sens. Actuators, A 282 (2018) 114–123.
[9] C. Yang, S. Chen, G. Yang, Fiber optical liquid level sensor under cryogenic environment, Sens. Actuators, A 94 (2001) 69–75.
[10] R. Kim, C.H. Park, W.J. Yoo, J.H. Moon, Development and characterization of a fiber-optic monitoring system for the key environment variables of the spent fuel pool at a nuclear power plant, Ann. Nucl. Energy 99 (2017) 183–192.
[11] C.A.F. Marques, A. Pospori, D. Sáez-Rodríguez, K. Nielsen, O. Bang, D.J. Webb, Fiber-optic liquid level monitoring system using microstructured polymer FBG array sensors, in: Proc. Of the 24th International Conference on Optical Fibre Sensors, 2013. Curitiba, Brazil, September 28-October 2.
[12] C. Teng, H. Liu, H. Deng, S. Deng, H. Yang, R. Xu, M. Chen, L. Yuan, J. Zheng, Liquid level sensor based on a V-Groove structure plastic optical fiber, Sensors 18 (2018), https://doi.org/10.3390/s18093111.
[13] D. Wang, Y. Zhang, B. Jin, Y. Wang, M. Zhang, Quasi-distributed optical fiber sensor for liquid-level measurement, IEEE Photonics J (2017), https://doi.org/10.1109/JPHOT.2017.2776245.
[14] H.-K. Lee, J. Choo, G. Shin, A simple all-optical water level monitoring system based on wavelength division multiplexing with an arrayed waveguide grating, Sensors 19 (2019), https://doi.org/10.3390/s19143095.
[15] C.-B. Kim, C.B. Su, Measurement of the refractive index of liquids at 1.3 and 1.5 micron using a fibre optic Fresnel ratio meter, Meas. Sci. Technol. 15 (2004) 1683–1686.
[16] K. Yüksel, Optical fiber sensor system for remote and multi-point refractive index measurement, Sens. Actuators, A 250 (2016) 29–34.
[17] Y.H. Kim, S.J. Park, S.-W. Jeon, S. Ju, C.-S. Park, W.-T. Han, B.H. Lee, Thermo-optic coefficient measurement of liquids based on simultaneous temperature and refractive index sensing capability of a two-mode fiber interferometric probe, Optic Express 20 (2012) 23744–23754.
[18] S.-R. Moon, H.-K. Lee, C.-H. Lee, Automatic wavelength Allocation method using Rayleigh backscattering for a WDM-PON with tunable lasers, J. Opt. Commun. Netw. 5 (2013) 190–197.
[19] Industry Guidance for Compliance with NRC Order EA-12-051, “To Modify Licenses with Regard to Reliable Spent Fuel Pool Instrumentation”, NEI 12-02 Rev.1, Nuclear Energy Institute, Washington DC, 2012.